DOI: 10.1002/ejoc.200700349

Chlorodifluorothioacetic Acid, $CF_2ClC(O)SH$: Synthesis, Characterization, X-ray Structure and Conformational Properties

Mauricio F. Erben,[a][‡] Roland Boese,[b] Helge Willner,[c] and Carlos O. Della Védova*[a,d][‡]

Keywords: Sulfur / Thiocarboxylic acids / Conformation analysis / Structure elucidation / Ab initio calculations

Chlorodifluoroacetic anhydride, $[CF_2ClC(O)]_2O$, and chlorodifluoroacetyl chloride, $CF_2ClC(O)Cl$, react with hydrogen sulfide to yield chlorodifluorothioacetic acid, $CF_2ClC(O)SH$. This novel thiocarboxylic acid has been obtained in pure form and characterized by NMR, IR and Raman spectroscopy. By extrapolation of the vapour pressure curve, $\log p = 6.102–2068/T$ (p [bar], T [K]), the boiling point was determined to be 66(1) °C. The melting point of the pure substance is –83(2) °C. The conformational properties of the gas-phase molecule have been studied by vibrational spectroscopy [IR (vapour), Raman (liquid)] and quantum chemical calculations [B3LYP and MP2 methods with 6-311++G(d,p) and 6-311++G(3df,2p) basis sets]. The most stable form has C_1 symmetry with a synperiplanar (*syn*) orientation of the C=O double bond with respect to the S–H single bond whereas in the chlorodifluoroacetyl group the *gauche* orientation of the ClC–C=O moiety is preferred (*gauche-syn* form). The analysis of the IR spectrum of gaseous $CF_2ClC(O)SH$ suggests the presence of two other conformations in equilibrium at room temperature. These forms have been fully characterized by high-level quantum chemical calculations. The structure of a single crystal, grown by a miniature zone-melting procedure using focused infrared laser radiation, was determined by X-ray diffraction analysis at low temperature. The crystalline solid [monoclinic, space group $C2/c$, a = 17.6165(14), b = 5.8848(5), c = 11.0877(9) Å, β = 113.5330(11)°] consists exclusively of molecules adopting the *gauche-syn* conformation. These molecules associate, forming pairs of cyclic dimers in the crystal through S–H···O=C hydrogen bonds.

Introduction

Thioacetic acid, $CH_3C(O)SH$, was first obtained in 1854 by Kekulé[1] and represents the first known organic acid containing sulfur.[2,3] Currently this compound is widely used in chemical synthesis as a reagent for the introduction of the thiol group into organic molecules, being the most common and versatile reagent for the free-radical addition of a thiol precursor to terminal alkenes.[4] Halothioacetic acids of the type $CX_3C(O)SH$ (X = halogen) are also very well known. For instance, the addition of trichlorothioacetic acid to olefins was studied early on by Cunneen.[5] More recently, $CCl_3C(O)SH$ has been used as a donor ligand to form stable gold(I) complexes.[6] With a similar purpose, the reactivity of group-12 metal thiocarboxylate species has been used to prepare valuable metal sulfide materials by thiocarboxylic anhydride elimination.[7] Trifluorothioacetic acid, $CF_3C(O)SH$, was prepared in 1960 by Sheppard and Muetterties[8] and its chemistry was further explored by Rochat and Gard.[9] As has been pointed out by these authors, the presence of the –SH group offers a way of preparing new sulfenyl halides and sulfides that contain the trifluoroacetyl group.

While the molecular structure and conformational properties of carboxylic acids have been widely studied, analogous thiocarboxylic species have attracted less attention. In principle, two planar conformations, with a *syn* and *anti* orientation of the C=O bond with respect to the S–H bond, are feasible for the –C(O)SH moiety (Scheme 1). At this point, $CH_3C(O)SH$ is by far the most-studied thiocarboxylic acid species. The molecular structure of gaseous $CH_3C(O)SH$ in its electronic ground state was studied early on by Gordy. By gas electron diffraction, the geometrical parameters of the heavy atoms could be estimated.[10] Furthermore, several studies of the vibrational spectra have been carried out with the aim of seeking evidence of a possible thiol/thione tautomeric equilibrium.[11,12] Noe[13] investigated the conformational equilibrium around the C–S

[a] CEQUINOR (CONICET-UNLP), Departamento de Química, Facultad de Ciencias Exactas, Universidad Nacional de La Plata,
47 esq. 115 (B1900AJL), C. C. 962, La Plata, Buenos Aires, República Argentina
Fax: +54-221-425-9485
E-mail: carlosdv@quimica.unlp.edu.ar
[b] Institut für Anorganische Chemie, Universität Duisburg-Essen, Universitätsstr. 5–7, 45117 Essen, Germany
[c] FB C, Anorganische Chemie, Bergische Universität Wuppertal, Gaußstrasse 20, 47097 Wuppertal, Germany
[d] Laboratorio de Servicios a la Industria y al Sistema Científico (UNLP-CIC-CONICET),
Camino Centenario, Gonnet, Buenos Aires, República Argentina
[‡] Mauricio F. Erben and Carlos O. Della Védova are members of the Carrera del Investigador of CONICET, República Argentina.

Supporting information for this article is available on the WWW under http://www.eurjoc.org or from the author.

bond in $CH_3C(O)SH$ by a temperature-dependence study of the ^1H NMR spectrum. The *syn* conformation is preferred over the *anti*, with a free-energy difference of 1.9 kcal mol^{-1} between the two rotamers. Recently, this equilibrium was also studied by matrix infrared spectroscopy experiments.[14] The results indicate that the vapour of $CH_3C(O)SH$ at ambient temperature consists of a mixture of the *syn* and *anti* conformers with the *syn* form predominating (ca. 85%). The electronic properties of valence- and inner-shell levels in $CH_3C(O)SH$ have also been studied.[15,16] An electron diffraction analysis of gaseous trifluorothioacetic acid; $CF_3C(O)SH$, complemented by quantum chemical calculations at the HF/6-31G* and MP2/6-31G* levels of theory, has also been reported.[17] The *syn* conformation seems to be again the preferred conformation, in agreement with the vibrational analysis reported earlier by Crowder.[18] Recently, Møllendal[19] reported the microwave spectra of $CF_3C(O)SH$ and of the deuteriated species $CF_3C(O)SD$. Only one rotamer was assigned. It appears that the –C(O)SH group is distorted somewhat from an exact synperiplanar arrangement, while the CF_3 group is rotated several degrees from a position in which one of the C–F bonds eclipses the C–S bond.

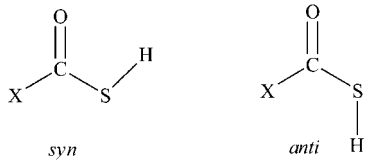

Scheme 1. Representation of the *syn* (left) and *anti* (right) conformers of XC(O)SH compounds.

In order to gain additional information about the structural and conformational behaviour of thioacetic acid derivatives, we became interested in the novel $CF_2ClC(O)SH$ species. In this paper, its synthesis and characterization are reported. The geometric structure and conformational properties have also been determined by experimental and theoretical methods.

Results and Discussion

Synthesis

To the best of our knowledge, the preparation of the simple chlorodifluorothioacetic acid has not been reported in the literature up to now. The synthesis of $CF_2ClC(O)SH$ was adapted from that reported by Sheppard and Muetterties[8] for $CF_3C(O)SH$, by treatment of either $CF_2ClC(O)Cl$ or $CF_2ClC(O)OC(O)CF_2Cl$ with H_2S at elevated pressures and temperatures (ca. 10 atm and 170 °C, respectively) in a metal autoclave, according to Equations (1) and (2), respectively.

$$CF_2ClC(O)Cl + H_2S \rightarrow CF_2ClC(O)SH + HCl \quad (1)$$

$$[CF_2ClC(O)]_2O + 2\,H_2S \rightarrow 2\,CF_2ClC(O)SH + H_2O \quad (2)$$

Conventional vacuum techniques were used to condense the acid chloride or the anhydride (typically 9 mmol) with a slight excess of H_2S with respect to the stoichiometric amounts indicated in Equations (1) and (2), respectively. The autoclave was allowed to reach ambient temperature and then placed in a glycerine bath at 170 °C. After the reaction mixture had been held at this temperature for 48 h, the volatile components were fractionated under dynamic vacuum through traps held at –50, –80 and –196 °C. $CF_2ClC(O)SH$ was collected in the –80 °C trap in yields of 45 and 40%, based on Equations (1) and (2) and the amount of $CF_2ClC(O)Cl$ or $[CF_2ClC(O)]_2O$, respectively. Some of the chemical properties of the new compound have been determined. Thus, $CF_2ClC(O)SH$ readily reacts at –60 °C with chlorine to give chlorodifluoroacetylsulfenyl chloride, $CF_2ClC(O)SCl$.[20] The formation of chlorodifluoroacetyl disulfides of the type $CF_2ClC(O)SSR$ also becomes feasible by the reaction of $CF_2ClC(O)SH$ with sulfenyl chlorides.[9] Thus, the title compound reacts quantitatively by Haas' chemistry with FC(O)SCl, ClC(O)SCl and CCl_3SCl to yield several new disulfides, $CF_2ClC(O)SSC(O)F$,[21] $CF_2ClC(O)SSC(O)Cl$ and $CF_2ClC(O)SSCCl_3$, respectively.[20,22]

Physical Properties and Spectroscopic Characterization

The new compound is a colourless liquid with the characteristic overpowering sulfenylcarbonyl odour. In the liquid and gaseous states, the compound is stable for days at room temperature. The vapour pressure over the temperature range 230–277 K follows the equation $\log p = 6.102 - 2068/T$ (p [bar], T [K]), and by extrapolation gives a boiling point of 329(1) K [66(1) °C]. The melting point of the pure substance is –83(2) °C.

In the ^{19}F and ^1H NMR spectra singlet signals are observed at –62.0 and 4.6 ppm, respectively. For the chlorodifluoroacetic acid analogue, $CClF_2C(O)OH$, the signal in the ^{19}F NMR spectra appears at –62.161 ppm.[23] The proton chemical shift value is close to that reported for the $CH_3C(O)SH$[13] and $CF_3C(O)SH$[9] thioacetic acids (5.44 and 5.2 ppm, respectively). The molecular weight, determined by Regnault's method, is 147(2) [$CF_2ClC(O)SH$ requires 146.5]. Additional evidence for the identity of $CF_2ClC(O)SH$ comes from the IR spectrum of the vapour and the Raman spectrum of the liquid, as discussed in the following sections.

Quantum Chemical Calculations

As has already been mentioned in the Introduction, depending on the torsional angle around the C–S bond, two planar conformations (*syn* and *anti*) are expected for thioacetic acid derivatives. Concerning the chlorodifluoroacetyl group, both *gauche* and *anti* orientations of the C–Cl single bond with respect to the C=O double bond were observed for the related molecule $CClF_2C(O)Cl$ in the vapour phase.[24,25] Thus, these antecedents suggest the occurrence of at least four possible forms of $CF_2ClC(O)SH$. In order to evaluate this forecast, relaxed potential energy curves were

obtained from calculations at the B3LYP/6-31G* level of theory. At first, the potential energy functions around the C–C bond were estimated by optimizing the molecular geometry every 20° for constant values of the ϕ(ClC–C=O) dihedral angle between 0 and 180° (Figure 1). In the corresponding potential energy function obtained for the optimizations of structures with a *syn* orientation of the ϕ(C=O–SH) dihedral angle (curve **A**), only one minimum occurs for a *gauche* structure with a ϕ(ClC–C=O) dihedral angle value close to 75° (this form is shown in Figure 2, referred to as *gauche-syn*). Another potential energy curve obtained between 0 and 180° with the ϕ(O=C–SH) dihedral angle set close to the *anti* orientation is also shown in Figure 1 (curve **B**). Two minima are now observed, the *gauche-anti* and *syn-anti* forms in Figure 2, which are higher in energy than the *gauche-syn* form. It is worth mentioning that both "*gauche*" minima (*gauche-syn* and *gauche-anti*) have quite different ϕ(ClC–C=O) dihedral angle values, as can be observed in Figure 2. When going from the *syn* to the *anti* orientation around the C–S bond, ϕ(ClC–C=O) changes from around 75° to around 95°. Thus, in the *gauche-syn* structure one C–F bond nearly eclipses the C–S bond, whereas in the *gauche-anti* conformer the C=O and the C–F bonds are nearly eclipsed. The relaxed potential energy curve around the C–S bond has also been calculated by optimizing the molecular geometry every 20° for constant values of the ϕ(O=C–SH) torsional angle between 0 and 180°. As anticipated, two minima appear in the potential energy curve (Figure 3) separated by around 2.1 kcal/mol, the *gauche-syn* conformer being more stable than the *gauche-anti* form. The same curve is obtained for input geometries corresponding to a *gauche* or *syn* orientation of the C–Cl and C=O bonds in the chlorodifluoroacetyl group.

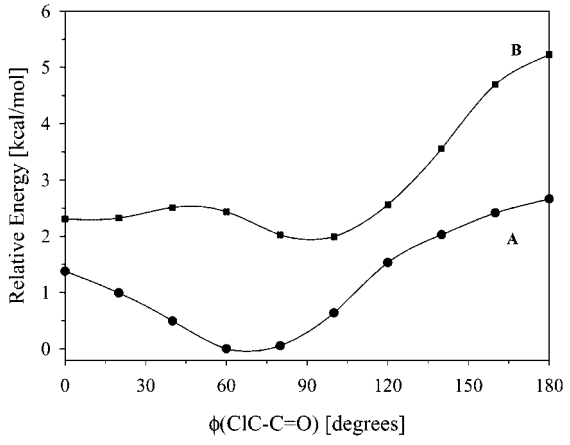

Figure 1. Calculated potential functions for internal rotation around the C–C bond in $CF_2ClC(O)SH$. In curves **A** and **B** the ϕ(O=C–SH) dihedral angle was optimized near values of 0 and 180°, respectively.

Additionally, full geometry optimizations and frequency calculations were carried out for each of the stationary structures [three minima and five transition states (TS)] at high levels of theoretical approximations, including the B3LYP and MP2 methods with the 6-311++G(d,p) and the extended 6-311++G(3df,2p) basis sets. Predicted relative energies corrected by zero-point calculations, $\Delta E°$, are gathered in Table 1. These calculations predict the existence of three stable forms of $CF_2ClC(O)SH$ separated by less than 1.6 kcal/mol. All the methods agree with the fact that the lower energy form corresponds to a conformer with a *gauche* and *syn* orientation of the C–Cl and the S–H bonds with respect to the C=O bond, respectively. The second stable form, higher in energy by around 0.65 kcal/mol ($\Delta E°$ values were calculated to be 0.63 and 0.67 kcal/mol by the B3LYP and MP2 methods, respectively) corresponds to a conformer with a *gauche* and *anti* orientation for the same dihedral angles, respectively. A third conformer with a *syn* and *anti* orientation of the C–Cl and S–H bonds with respect to the C=O bond, respectively, also results in a minimum in the potential hypersurface, located at around 1.2 kcal/mol above the minimum-energy conformer.

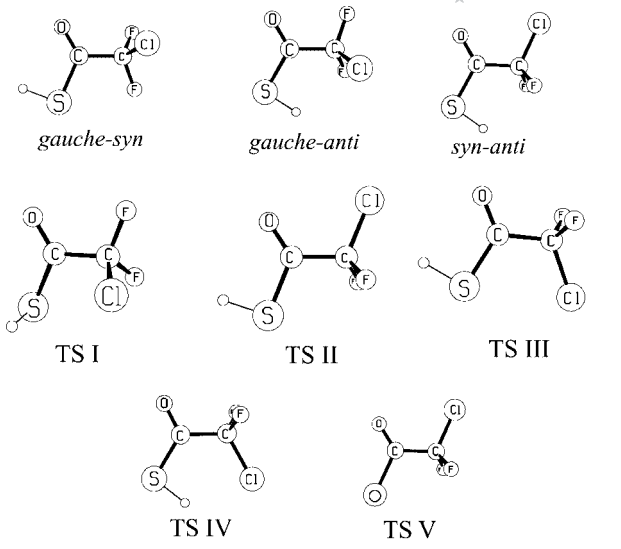

Figure 2. Molecular models for stationary-point structures of $CF_2ClC(O)SH$.

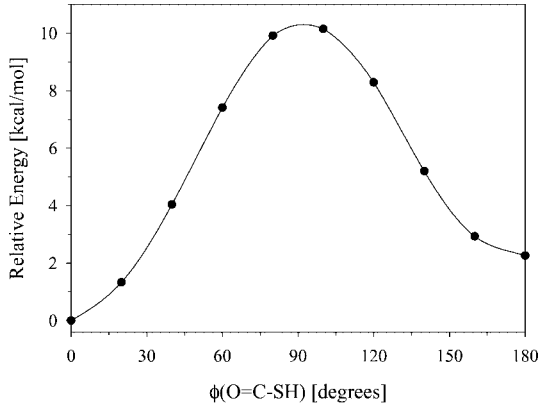

Figure 3. Calculated potential function for internal rotation around the C–S bond in $CF_2ClC(O)SH$.

Two species with C_s global symmetry with a *syn* [ϕ(ClC–C=O) = 0°] and *anti* [ϕ(ClC–C=O) = 180°] orientation of the C–Cl and C=O bonds, respectively, correspond to max-

Table 1. Calculated relative energies [kcal/mol] (corrected by zero-point calculations) for the stationary structures of $CF_2ClC(O)SH$.

		gauche-syn	*gauche-anti*	*syn-anti*	$TS_{gauche\text{-}gauche}$	$TS_{syn\text{-}syn}$	$TS_{anti\text{-}syn}$	$TS_{syn\text{-}gauche}$	$TS_{anti\text{-}anti}$
B3LYP	6-311++G(d,p)	0.00[a]	0.86	1.43	8.71	1.28	1.99	9.32	4.11
	6-311++G(3df,2p)	0.00[b]	0.67	1.24	8.25	1.25	1.76	9.53	3.52
MP2	6-311++G(d,p)	0.00[c]	0.98	1.58	8.27	1.33	2.41	8.83	4.91
	6-311++G(3df,2p)[d]	0.00[e]	0.63	1.15	–	–	–	–	–

[a] $E°$ = –1210.229399 hartree. [b] $E°$ = –1210.264162 hartree. [c] $E°$ = –1208.308707 hartree. [d] Zero-point corrections calculated at the MP2/6-311++G(d,p) level of theory; transition-state structures were not calculated at the MP2/6-311++G(3df,2p) level of theory. [e] E = –1208.6321075 hartree.

ima in the potential energy curve. These forms were characterized as the TSs (N_{imag} = 1) connecting enantiomeric *gauche* structures with ϕ(ClC–C=O) ≈ ±75°. Molecular diagrams of these forms are shown in Figure 2 (TS II and TS III, respectively). It is worth mentioning that the corresponding structures with a *syn* orientation around both the C–C and C–S dihedral angles are also characterized as torsional TSs. In effect, the calculated [B3LYP/6-311++G(3df,2p)] barrier heights, corrected zero-point energies, for the planar TS II and TS III are 1.25 and 1.76 kcal/mol, respectively (Table 1). The TS IV structure shown in Figure 2 corresponds to a high-energy TS for torsional interconversion around the C–C single bond. The structure calculated for the near-perpendicular orientation of the thiocarboxylic group [ϕ(O=C–SH) = 90°] is also characterized as a TS connecting the *syn* and *anti* forms by internal rotation. Indeed, two structures that correspond to torsional TSs were found for the *gauche-syn* → *gauche-anti* conformational transition. These forms have a near-perpendicular orientation of the ϕ(O=C–SH) dihedral angle and either a *syn* or *gauche* orientation of the C–Cl and the C=O bonds. Calculations at the B3LYP/6-311++G(3df,2p) level of theory predict a height barrier of 8.25 (TS I) and 9.53 kcal/mol (TS V), respectively, values which are in the range of those reported for thioesters.[26,27]

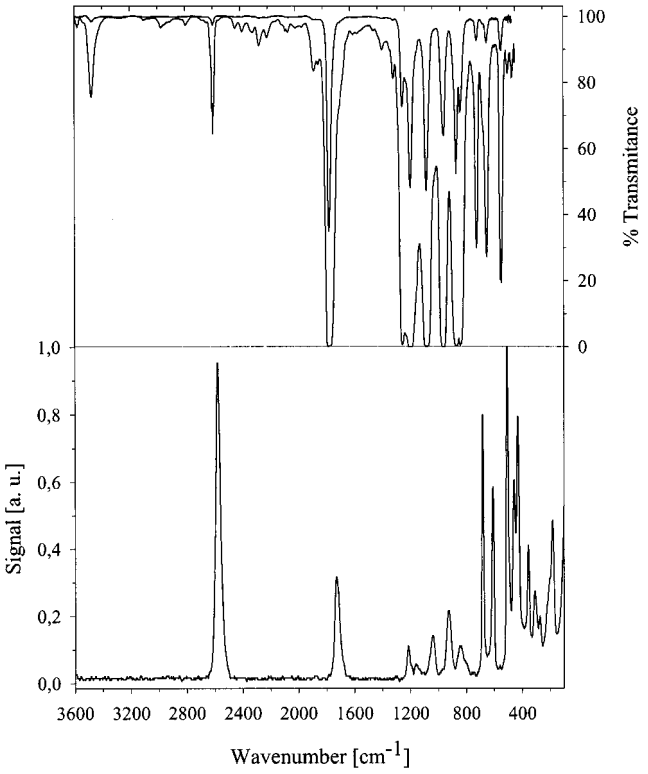

Figure 4. Gas IR spectra at 2.0 and 28.1 mbar (top; glass cell, 200 mm optical path length, Si windows, 0.5 mm thick) and liquid Raman spectra for $CF_2ClC(O)SH$ (bottom).

Vibrational Spectra

The IR (vapour) and Raman (liquid) spectra of $CF_2ClC(O)SH$ are shown in Figure 4. A tentative assignment of the observed bands was performed by comparison with calculated spectra and the description of modes is based on the calculated displacement vectors of the fundamentals as well as on comparison with spectra of related molecules, especially $CF_3C(O)SH$[18,28] and $CF_2ClC(O)Cl$.[24] Furthermore, the potential energy distribution (PED) associated with each normal vibrational mode under the harmonic assumption was calculated. Experimental and calculated [B3LYP/6-311++G(3df,2p)] frequencies, intensities and their tentative assignments are given in Table 2. In view of the rich conformational behaviour envisaged by the quantum chemical calculations, a quite detailed analysis of the vibrational spectra has been carried out in order to assess the presence of conformers of $CF_2ClC(O)SH$ in the gaseous phase. Structural changes should affect specific force constants for each conformer, making possible their identification in the vibrational spectra.

The strongest band in the IR spectrum of the vapour centred at 1753 cm^{-1} is assigned to the C=O stretching mode. The vibrational spectra of thioacetic acid derivatives were found to be very similar to those of its acetyl chloride counterparts.[18] In effect, as noted by Crowder et al.,[29] the C–S[30] and C–Cl[31] force constants are almost the same and since the masses of the sulfur and chlorine atoms are similar, the C(sp^2)–S and C(sp^2)–Cl stretching frequencies in $CF_2ClC(O)SH$ (459 cm^{-1}, Raman) and $CF_2ClC(O)Cl$ (456 cm^{-1}, Raman)[24] are about the same. However, the ν(C–S) stretching modes reported for similar thiocarboxylic acids, such as $CF_3C(O)SH$ and $CH_3C(O)SH$, are considerably higher: 747 (IR, vapour)[18] and 615 cm^{-1} (IR, matrix),[14] respectively. Hence, the frequency at 454 cm^{-1} proposed for ν(C–S) seems to be a fairly low value for a C(sp^2)–S stretching mode. In order to obtain a complete description of the molecular motions involved in the normal modes of $CF_2ClC(O)SH$, a normal coordinate analysis was

Table 2. Observed and calculated vibrational data [cm^{-1}] for $CF_2ClC(O)SH$.

Experimental IR[a]	Raman[b]	Calculated[c] *gauche-syn*	*gauche-anti*	*syn-anti*	Assignment/approximated description of mode (PED)[d]
3584					$\nu_1 + \nu_5$
3478 (2.0)					$2 \times \nu_2$
2797					$\nu_2 + \nu_5$
2434					$\nu_3 + \nu_4$
2311					$2 \times \nu_4$
2051					$2 \times \nu_5$
2618 sh 2596 (2.8)[e]	2580 (94.7)	2677 (1.5)	2696 (1.0)	2680 (1)	ν_1/ν(S–H) (100)
1753 (100)	1730 (32.0)	1801 (100)[c]	1799 (100)[c]	1807 (94)	ν_2/ν(C=O) (100)
1220 (31.6)	1215 (8.1)	1205 (30.2)	1208 (25.4)	1163 (43)	ν_3/ν(C–C) (40) + ν_s(C–F) (35) + ν_{as}(C–F) (10)
1161 (73.6)	1168 (3)	1152 (65.0)	1141 (55.7)	1092 (72)	ν_4/ν_{as}(C–F) (90)
1046 (74.7)	1040 (10.8)	1026 (55.5)	1041 (61.2)	1074 (39)	ν_5/ν_s(C–F) (50) + δ(C–S–H) (20) + ν(C–Cl) (10)
919 (45.1)	929 (17.5)	917 (31.9)	915 (39.9)	953 (49)	ν_6/δ(C–S–H) (50) + ν(C–Cl) (20) + CF_2 wag (20)
829 (62.7) 800 (34.0)	846 (7.0)	822 (86.5)	837 (53.0)	783 (100)[c]	ν_7/CF_2 wag (35) + ν(C–S) (25) + δ(CSH) (20)
681 (7.9)	682 (85.5)	683 (6.5)	684 (5.8)	695 (1)	ν_8/oop (C=O) (30) + $\delta_s(CF_2Cl)$ (15)
639 sh 608 (8.8)[f]	609 (56.7)	603 (11.2)	600 (7.5)	668 (<0.1)	ν_9/ν(C–Cl) (40) + oop (C=O) (35) + CF_2 def (20)
501 (10.4)[f]	508 (100)	508 (6.6)	495 (3.6)	481 (3)	ν_{10}/δ(SCO) (30) + CF_2 def (20) + ρ_s (CF_2Cl) (20)
454 (2.0)	459 (17.3)	455 (0.8)	450 (1.0)	433 (0.1)	ν_{11}/ν(C–S) (45) + ρ_s (CF_2Cl) (25)
427 (2.5)	429 (55.4)	420 (0.1)	419 (0.2)	397 (<0.2)	ν_{12}/ν(C–Cl) (40) + δ_s (CF_2Cl) (40)
		394 (4.7)	351 (0.3)	379 (<0.1)	ν_{13}/τ(C–S)
	355 (25.9)	352 (0.3)	329 (3.2)	321 (3)	ν_{14}/ρ_{as} (CF_2Cl) (40) + ρ (C=O) (20) + CF_2 twist (20)
	310 (12.5)	296 (0.7)	306 (0.6)	264 (0.2)	ν_{15}/CF_2 twist (65) + δ(S–C=O) (15)
	273 (4.7)	198 (0.7)	216 (1.6)	230 (2)	ν_{16}/δ(SC=O) (60) + $\rho_{as}(CF_2Cl)$ (30)
	180 (30.1)	177 (0.05)	168 (0.8)	180 (2)	ν_{17}/CCCl def (90)
		34 (0.3)	37 (0.8)	25 (1)	ν_{18}/τ(C–C) (100)

[a] Relative absorbance at band maximum are given in parentheses; gas phase, glass cell 200 mm optical path length, Si windows, 0.5 mm thick. [b] Relative absorbance at band maximum are given in parentheses; liquid, room temperature. [c] B3LYP/6-311++G(3df,2p) method, relative band strengths are given in parentheses; 100% ≡ 265.8, 288.0 and 251.3 km/mol for the *gauche-syn*, *gauche-anti* and *cis-anti* conformers, respectively. [d] Calculated for the *gauche-syn* conformer with the B3LYP/6-311++G(3df,2p) method. The internal coordinates are defined in the Supplementary Information. Contributions of less than 10% have been omitted. [e] PQR-structured A-type band centred at 2596 cm^{-1} with a PR separation equal to 10 cm^{-1}. [f] PR-structured B-type band with a PR separation equal to 7 cm^{-1}.

carried out. From the PED analysis, the S_{10} symmetry coordinate, which mainly describes the C–S stretching mode (see Table S5 and Figure S1 given as electronic supporting information), is predicted to contribute 45 and 25% to the predicted fundamental modes at 455 and 822 cm^{-1} [B3LYP/6-311++G(3df,2p)], respectively. Thus, the internal coordinate related to C–S stretching seems to be highly mixed between these normal modes of $CF_2ClC(O)SH$.

The ν_{as}(C–F) and $\nu(F_2C–Cl)$ normal modes of vibration for $CF_2ClC(O)Cl$ are 1188 and 607 cm^{-1}, respectively,[24] whereas for the title compound, the bands located at 1161 and 608 cm^{-1} were assigned to these modes, respectively. The δ(CSH) deformation mode is assigned to the 919 cm^{-1} absorption observed in the IR spectra (929 cm^{-1} liquid Raman). This mode appears at 860 and 874 cm^{-1} in the IR and Raman spectra of $CF_3C(O)SH$, respectively,[18,28] whereas for $CH_3C(O)SH$ it occurs at 820 (IR, matrix)[14] and 830 cm^{-1} (IR, vapour).[12]

Some controversies exist about the assignment for the ν(C–C) and ν_s(C–F) stretching modes in difluorohaloacetyl species [$CF_2XC(O)$–, X = halogen]. For instance, for $CF_2ClC(O)Cl$, Durig et al.[24] assigned the bands located at 1017 and 1188 cm^{-1} to these modes, respectively, whereas for $CF_3C(O)SH$, Crowder et al.[18,29] reversed the assignment, the higher frequency band (1286 cm^{-1}) being assigned to the ν(C–C) and the absorption at 1032 cm^{-1} to the $\nu_s(CF_3)$ mode. In agreement with the PED obtained for the title compound, these two normal modes of vibration are formed by highly mixed sets of symmetry coordinates. Therefore, we tentatively assign the high frequency band observed at 1220 cm^{-1} to the ν(C–C) stretch, while the absorption observed at 1046 cm^{-1} is assigned to the ν_s(C–F) mode. For $CH_3C(O)SH$, the bands located at 1127 and 1128 cm^{-1} in the matrix and vapour IR spectra, respectively, were assigned to the ν(C–C) normal mode.[14]

Most of these features observed in the vibrational spectra are well reproduced by standard quantum chemical calculations for the more abundant *gauche-syn* form (Table 2). An enlargement of the 2750–2450 cm^{-1} region of the IR (vapour) spectrum of $CF_2ClC(O)SH$ is shown in Figure 5 (trace **B**). The A-type absorption centred at 2596 cm^{-1}, with a PR separation of 10 cm^{-1}, is assigned to the ν(S–H) stretching mode of the *gauche-syn* conformer, while a shoulder observed at higher frequencies (ca. 2618 cm^{-1}) could be due to the presence of the less stable *gauche-anti* form. This assignment is in agreement with quantum chemical calculations. In effect, the ν(S–H) stretching mode can be seen as a conformational sensor for the molecule. The main frequency divergence expected from the calculated IR spectra of both the *gauche-syn* and *gauche-anti* conformers falls on

the ν(S–H) stretching mode, with a value of 19 cm^{-1}. The simulated spectra for the weighted mixture of the three stable forms obtained from frequency calculations at the B3LYP/6-311++G(3df,2p) level of theory is shown in trace **A** of Figure 5. The enlargement of the ν(S–H) stretching region shows a very similar feature when compared with the experimental spectrum. Vertical bars indicate the ν(S–H) frequencies calculated for the three forms.

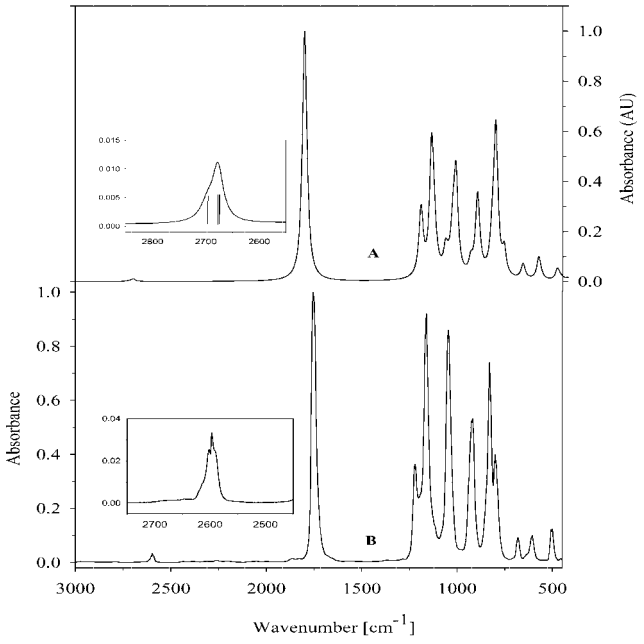

Figure 5. Simulated IR spectrum calculated at the B3LYP/6-311++G(3df,2p) level of theory for a mixture of three stable conformers (trace A) and the vapour IR spectrum (2.0 mbar) for $CF_2ClC(O)SH$ (trace B). The insets show enlargements of the ν(S–H) stretching region, with vertical bars indicating the frequency values calculated for the three forms.

Durig et al.[24] studied the conformational equilibrium between the *gauche* and *anti* conformers of $CF_2ClC(O)Cl$ (F_2C–Cl bond oriented in the *gauche* and *anti* position with respect to the terminal C–Cl bond, respectively) by using vibrational spectroscopy techniques. The analysis of the CF_2 deformation mode (wagging) results being especially suitable for this purpose because two absorptions at 862 and 810 cm^{-1} were identified as belonging to each form, respectively. For $CF_2ClC(O)SH$ only one absorption is expected at around 800 cm^{-1}. Nevertheless, two bands with strong and medium intensity appear in this region at 829 and 800 cm^{-1}, respectively. The values calculated for the *gauche-syn* and *gauche-anti* forms are 822 and 837 cm^{-1}, respectively. Thus, while the most intense of these bands (829 cm^{-1}) can be assigned with confidence to the more stable *gauche-syn* form, it is unlikely that the *gauche-anti* conformer creates the absorption at 800 cm^{-1}, a frequency value lower than that of the former form. Frequency calculations performed for the third stable *syn-anti* conformation [B3LYP/6-311++G(3df,2p)] predict the CF_2 deformation mode to be the most intense IR absorption at 783 cm^{-1} (Table 2), 39 cm^{-1} lower than that calculated for the *gauche-syn* form. In this way, comparison with the calculated frequencies allows the assignment of the 800 cm^{-1} band to the *syn-anti* conformer. According to our calculations, other fundamental modes of these three conformers either differ by less than 5 cm^{-1} or present too weak an intensity to be observed in the spectra. The experimental IR spectrum of vapour $CF_2ClC(O)SH$ and the spectrum calculated for a mixture of the three stable forms are included in Figure 5 for comparative purposes. The agreement between them is remarkable.

Crystal Structure

Chlorodifluorothioacetic acid crystallizes in the monoclinic space group *C*2/*c* with eight $CF_2ClC(O)SH$ molecules per unit cell (for all the crystallographic data and treatment information see Table S1 of the Supplementary Information). Only the *gauche-syn* conformer is observed in a single crystal of $CF_2ClC(O)SH$ at 169 K. The thiocarboxylic moiety exhibits the following structural parameters: the C=O and C–S bond lengths are 1.202(3) and 1.742(3) Å, respectively, and the S–C=O, C–C–S and O=C–C bond angles are 127.42(18), 113.5(17) and 119.1(2)°, respectively. The *gauche* orientation of the Cl–C bond with respect to the C=O double bond is observed in the crystal with a ϕ(ClC–C=O) dihedral angle of 83.2(3)°. The structure of the molecule is shown in Figure 6 and Table 3 includes the main geometric parameters derived from the structure refinement as well as those obtained from quantum chemical calculations. Little crystallographic information is available on thiocarboxylic acids. To the best of our knowledge, only the crystal structure of the substituted thiobenzoic acid 2-$HOC_6H_4C(O)SH$ (2-hydroxythiobenzoic acid) has been reported in detail [T = 200 K, $P2_1/a$, a = 14.903(5), b = 5.203(3), c = 9.114(6) Å, β = 92.40(4)°],[36] while for the similar 4-$CH_3C_6H_4C(O)SH$ hardly any crystallographic data have been reported.[37] Selected geometrical parameters experimentally determined for 2-$HOC_6H_4C(O)SH$ are also collected in Table 3. Similar values are found for both $CF_2ClC(O)SH$ and 2-$HOC_6H_4C(O)SH$. Deviations, such as those observed for the O=C–S bond angle, originate from the O–H···O=C intramolecular interaction present in 2-$HOC_6H_4C(O)SH$, clearly absent in the title molecule.

The two computational methods used predict dihedral angles for the molecular skeleton to be similar to those obtained from the X-ray analysis. Actually, the structure of the chlorodifluoroacetyl group is better described by the MP2 method, with ϕ(ClC–C=O) = 82.2°, while the B3LYP method gives a value of 78.8° which is slightly lower than the experimental one [ϕ(ClC–C=O) = 83.2(3)°]. Both methods reproduce the bond angles very well. The reproduction of the bond lengths around the sulfur and chlorine atoms is not quite so good. Thus, even with large basis sets [6-311++G(3df,2p)], the B3LYP method predicts the S–C and C–Cl bonds to be too long by 0.038 and 0.044 Å, respectively. Indeed, these bonds are better described by the MP2 method, with differences of only 0.019 and 0.018 Å, respec-

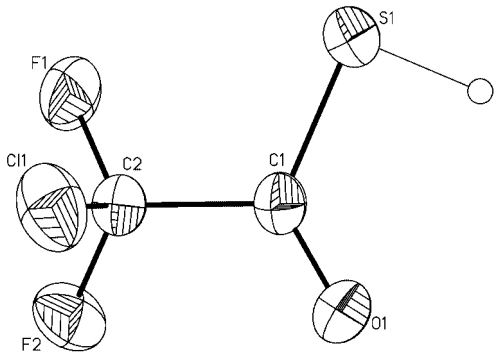

Figure 6. Molecular model with atomic numbering for the single-crystal structure of $CF_2ClC(O)SH$ at 169 K.

Table 3. Experimental and calculated geometric parameters for $CF_2ClC(O)SH$ and 2-hydroxythiobenzoic acid.[a]

	X-ray[b]	B3LYP[c]	MP2[c]	2-$HOC_6H_4C(O)SH$[b,d]
C=O	1.202(3)	1.193	1.203	1.211(5)
C–S	1.742(3)	1.780	1.761	1.776(3)
C–C	1.541(3)	1.558	1.547	1.483(5)
S–H	1.33(4)	1.344	1.338	1.40(4)
C–Cl	1.735(3)	1.779	1.753	
$(C–F)_{mean}$	1.347(3)	1.340	1.336	
O=C–S	127.42(18)	126.2	126.6	120.8(3)
O=C–C	119.1(2)	120.6	120.5	123.0(3)
C–C–S	113.5(17)	113.2	112.9	116.2(3)
C–S–H	90(2)	92.5	91.9	93(1)
C–C–Cl	109.02(18)	109.6	109.0	
$(C–C–F)_{mean}$	111.8(2)	110.4	110.2	
$(Cl–C–F)_{mean}$	109.35(19)	109.7	108.7	
F–C–F	105.4(2)	108.0	108.2	
ϕ(ClC–C=O)	83.2(3)	78.8	82.2	
ϕ(O=C–CF1)	155.3(2)	160.8	157.6	
ϕ(O=C–CF2)	–37.4(4)	–41.6	–38.3	

[a] Bond lengths are given in Å and angles in degrees. See Figure 6 for the atomic numbering. [b] The error limits given in parentheses are σ values. [c] *gauche-syn* form, 6-311++G(3df,2p) basis sets. [d] See ref.[36]

tively. Thus, allowing for the contraction of polar bonds, which is to be expected in practice on crystallization, both methodologies reproduce satisfactorily the molecular dimensions of the crystalline solid.

Although S–H is a relatively weak proton donor group, a number of thiols showing intramolecular hydrogen bonding have been studied.[32–34] Moreover, it was suggested earlier by Crowder[18] that the *syn* conformer of $CF_3C(O)SH$ is the preferred form because this rotamer would be stabilized by a H···F intramolecular hydrogen bond. For $CF_2ClC(O)SH$, the non-bonding distance between the hydrogen [–C(O)SH] and the nearest fluorine atom in a crystal is 2.749(4) Å, larger than 2.55 Å, the sum of the van der Waals radii.[35] Another hydrogen-bonding interaction between the hydrogen atom of the S–H group and the carbonyl oxygen atom might also be possible. The calculated [B3LYP/6-311++G(3df,2p)] non-bonding distance between the two atoms is 2.57 Å, which is slightly shorter than the sum of the van der Waals radii of hydrogen and oxygen (2.60 Å). Thus, intramolecular hydrogen bonding would have a small effect on the conformational properties of $CF_2ClC(O)SH$.

The molecules of $CF_2ClC(O)SH$ form hydrogen-bonded cyclic dimers just as in solid $CF_2ClC(O)OH$, the oxygen analogue.[38] The crystal packing, as viewed along the *ac* plane, is shown in Figure 7. The value of the intermolecular C=O···S(H)–C short contact is 3.490(4) Å, with an O···H hydrogen-bond length of 2.20(3) Å. The O···H–S angle is 162(2)°, more removed from linearity than the O···H–O moiety found in $CF_2ClC(O)OH$ to have an angle of 170(2)°. Thus, a weak hydrogen-bonding intermolecular interaction is observed in the sulfur analogue. This could be related to the differences in the molecular geometry of the monomeric units. In effect, while geometrical parameters around the sp^2 carbon atom are very similar when comparing the carboxylic and thiocarboxylic moieties, the C–O–H and C–S–H bond angles in $CF_2ClC(O)OH$ and $CF_2ClC(O)SH$ are rather different: 111(2) and 90(2)°, respectively. Thus, sp^3-type hybridization describes the bonds around the oxygen atom in the O–H group, whereas a canonical p orbital character is formally present in the S–H bond. Linearity of the C=O···X–H (X = O or S) hydrogen bond is then facilitated in the carboxylic acid derivative, making more efficient the intermolecular interaction. Similar differences between the cyclic dimers of the carboxylic and thiocarboxylic acids were found for 2-$HOC_6H_4C(O)OH$ and 2-$HOC_6H_4C(O)$-SH.[36]

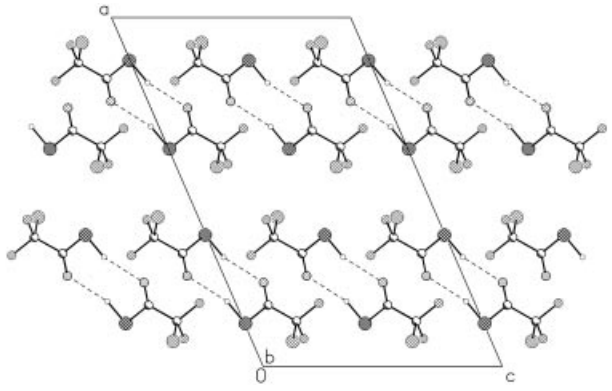

Figure 7. Stereoscopic illustration of the crystal packing of $CF_2ClC(O)SH$ at 169 K.

Beside the hydrogen bonds between the thiocarboxylic groups of pairs of monomers, other intermolecular interactions seem to be absent. The short distance between the chlorine atoms of different dimers [3.652(4) Å] is longer than the sum of the van der Waals radii of chlorine (ca. 3.52 Å).[35]

Conclusions

Rotational isomerism in haloacetyl halides is quite interesting as the more stable conformer may be either the *anti* or the *gauche* rotamer, depending on both the nature of the chemical environment of the C–C bond and the state (vapour, liquid or solid) under consideration[39–45] Of particular

interest for the present study, the more stable conformer of the chlorodifluoroacetyl chloride derivative, $CClF_2C(O)Cl$, in both fluid phases as well as in the annealed solid,[24] is the *gauche* rotamer, as deduced from experimental and theoretical methods.[25] The conformational properties of sulfenylcarbonyl compounds, with a general formulae XC(O)SY, have also been studied and the preference for a synperiplanar conformation around the C–S bond has been well-established.[46–50] In particular, conformational studies of thiocarboxylic species, such as $CH_3C(O)SH$ and $CF_3C(O)SH$, show a *syn* orientation of the C=O and S–H bonds.[14,17] According to vibrational spectroscopy, $CF_2ClC(O)SH$ exists in the gas phase at room temperature as a mixture of three conformers. The most stable form has a *gauche* and *syn* orientation of the chlorodifluoroacetyl and the thiocarboxylic moiety, respectively. Quantum chemical calculations reproduce the existence of two other conformations, characterized by the adoption of an *anti* orientation of the C=O and S–H bond and either a *gauche* or *syn* orientation of the C–Cl and C=O bonds. From calculated $\Delta G°$ values, and taking into account the different conformer degenerations, contributions of around 24 and 5% for the *gauche-anti* and *syn-anti* forms, respectively, could be expected to be present at room temperature.

The crystal structures of carboxylic acids have been extensively discussed by Leiserowitz.[51] It is established that in monocarboxylic acids the hydroxy group that does not participate in an intramolecular bond adopts a *syn* conformation [ϕ(O=C–O–H) = 0°] in the crystal. In particular, the crystal structure of acetic acid is built from chains of *syn* molecules which form the so-called "catemer" motif.[52] Together with formic acid, acetic acid is the only case in which a monocarboxylic acid does not crystallize as cyclic dimers.[53] The oxygen analogue of the title molecule, $CF_2ClC(O)OH$, also crystallizes forming cyclic dimers in which each of the two molecules form dimers through O–H···O=C hydrogen bonds. Following this trend, crystals of $CF_2ClC(O)SH$ are formed as cyclic dimers bonded by S–H···O=C weak hydrogen-bond-type interactions.

Experimental Section

General Procedure: Volatile materials were manipulated in a glass vacuum line equipped with two capacitance pressure gauges (221 AHS-1000 and 221 AHS-10, MKS Baratron, Burlington, MA), three U traps and valves with PTFE stems (Young, London, UK). The vacuum line was connected to an IR cell (optical path length 200 mm, Si windows, 0.5 mm thick) contained in the sample compartment of an FTIR instrument (Impact 400D, Nicolet, Madison, WI). This allowed us to monitor the purification processes and to follow the course of the reactions. The pure compound was stored in flame-sealed glass ampoules under liquid nitrogen in a long-term Dewar vessel. The ampoules were opened with an ampoule key on the vacuum line, an appropriate amount of the compound was taken out for the experiments and then the ampoules were flame-sealed again.[54]

Molecular Weight: The molecular weight of the compound was calculated from the vapour density, assuming ideal gas behaviour. The vapour density was determined using a thin-walled round-bottomed flask with a 6 mm glass valve with a PTFE stopcock.

Vapour Pressure and Melting Point: The vapour pressure of the sample was measured in a small vacuum line (volume ca. 15 mL) equipped with a capacitance manometer (MKS Baratron, AHS-100), a sample reservoir and a connecting tube to an IR gas cell. The temperature of the sample reservoir was adjusted with a series of ethanol cold baths and measured with a Pt-100 resistance thermometer. When the temperatures were constant, the resulting vapour pressures were determined. Occasionally, the gas phase was checked through its IR spectrum. No decomposition was detected during the whole measurement. The melting point was determined for a small, tensimetrically pure sample of the compound contained in a 6 mm o.d. glass tube immersed in cold ethanol in a transparent Dewar vessel; the temperature was measured with a small Pt-100 resistance sensor (Hereaus) attached to the sample tube.

Vibrational Spectroscopy: Gas-phase infrared spectra were recorded at a resolution of 1 cm^{-1} in the range 4000–400 cm^{-1} with a Bruker IFS 66v FTIR instrument and the FT-Raman spectra of liquid $CF_2ClC(O)SH$ with a Bruker RFS 100/S FT Raman spectrometer. The sample in a 4 mm glass capillary was excited with 500 mW of a 1064 nm Nd:YAG laser (ADLAS, DPY 301, Lübeck, Germany).

NMR Spectroscopy: For the ^{19}F and ^{1}H NMR measurements, neat samples were flame-sealed in thin-walled 3 mm o.d. tubes and placed in 5 mm NMR tubes. The spectra were recorded with a Bruker Avance DRX-300 spectrometer operating at 282.41 MHz. The sample was measured at room temperature using a mixture of CD_3CN and $CFCl_3$ as an external lock and reference.

X-ray Diffraction at Low Temperature: An appropriate crystal of $CF_2ClC(O)SH$ (ca. 0.3 mm diameter) was placed on the diffractometer at a temperature of 169 K with a miniature zone melting procedure using focused infrared laser radiation.[55,56] The diffraction intensities were measured at low temperatures on a Siemens SMART CCD area detector system. Intensities were collected with graphite-monochromated Mo-K_α radiation using the ω-scan technique. The crystallographic data, conditions and some features of the structure are listed in Table S1 of the Supplementary Information. The structure was solved by Patterson syntheses and refined by full-matrix least-squares methods on F using the SHELXTL-Plus program.[57] Absorption correction details are given elsewhere. All atoms were assigned anisotropic thermal parameters. Atomic coordinates and equivalent isotropic displacement coefficients are given in Table S2 and the anisotropic displacement parameters for $CF_2ClC(O)SH$ are given in Table S3 (see electronic supporting information). Hydrogen coordinates and isotropic displacements are given in Table S4.

Further details of the crystal structure investigation may be obtained from Fachinformationszentrum Karlsruhe, 76344 Eggenstein-Leopoldshafen, Germany [Fax: (+49)7247-808-666; E-mail: crysdata@fiz-karlsruhe.de, http://www.fiz-karlsruhe.de/ecid/Internet/en/DB/icsd/depot_anforderung.html] on quoting the deposition number CSD-417530.

Theoretical Calculations: All quantum chemical calculations were performed with the GAUSSIAN 03 program package.[58] MP2 and B3LYP methods were employed with standard basis sets up to the extended valence triple-ξ basis set augmented with diffuse and polarization functions for both hydrogen and non-hydrogen atoms [6-311++G(3df,2p)]. This basis set has been shown to be near the basis set saturation limit when used with the B3LYP functional.[59] Gradient techniques were used for the geometry optimizations and vibrational calculations, while transition states were optimized by

the synchronous transit-guided quasi-Newton (STQN)[60] method and torsional barrier heights were calculated from the relative energies of the TSs and the stable structures, taking into account the zero-point energies of the species. All the computed TS structures show only one imaginary frequency, which corresponds to the torsion involved in the conformational transition. For the normal coordinate analysis, transformations of the ab initio Cartesian harmonic force constants to the molecule-fixed internal coordinate system were performed, as described by Hedberg and Mills and implemented in the ASYM40 program.[61] By using this procedure the potential energy distribution (PED) associated with each normal vibrational mode under the harmonic assumption can be evaluated. The internal and symmetry coordinates used to perform the normal coordinate analysis are defined in Figure S1 and Table S5, respectively, provided as Supporting Information.

Chemicals: Chlorodifluoroacetic anhydride (98% Aldrich) was obtained from commercial sources, purified by trap-to-trap reduced-pressure distillation and stored in an ampoule with a Young valve over P_2O_5 (Fluka). Hydrogen sulfide (99.8%, Linde, Germany) was obtained from commercial sources and used without further purification. $CF_2ClC(O)Cl$[62] was obtained by the reaction between dry chlorodifluoroacetic acid, $CF_2ClC(O)OH$ (98%, Merck), and phosphorus pentachloride, PCl_5 (99%, Riedel-de Haën), and was subsequently purified several times by fractional condensation at reduced pressure.

Supporting Information (see also the footnote on the first page of this article): X-ray crystallographic data and structure refinement details, atomic coordinates and equivalent isotropic displacement parameters, and anisotropic displacement parameters. Symmetry and internal coordinate definition used in the normal coordinate analysis.

Acknowledgments

Financial support by the Volkswagen-Stiftung and the Deutsche Forschungsgemeinschaft is gratefully acknowledged. The Argentinean authors thank the ANPCYT-DAAD for German-Argentinean cooperation Awards (PROALAR). They also thank the Agencia Nacional de Promoción Científica y Tecnológica (ANPCYT), the Consejo Nacional de Investigaciones Científicas y Técnicas (CONICET), the Comisión de Investigaciones Científicas de la Provincia de Buenos Aires (CICBA) and the Facultad de Ciencias Exactas, Universidad Nacional de La Plata for financial support. M. F. E. and C. O. D. V. would like to express their gratitude to H. Pernice, P. García, M. Finze, S. Balters and S. von Ahsen for their friendship and invaluable help in the laboratory work during their stay in Duisburg. C. O. D. V. especially acknowledges the DAAD which generously sponsors the DAAD Regional Program of Chemistry for the República Argentina, supporting Latin-American students to study for their Ph.D.s in La Plata.

[1] A. Kekule, *Ann. Chem. Pharm.* **1854**, *90*, 309–311.
[2] M. J. Nye, *Before Big Science*, Twayne Publishers, New York, **1996**.
[3] R. Anschütz, *Biographical dictionary of Chemists*, August Kékule in *Great Chemists* (Ed.: E. Farber), Interscience, New York, London, **1961**.
[4] D. Witt, R. Klajn, P. Barski, B. A. Grzybowski, *Curr. Org. Chem.* **2004**, *8*, 1763–1795.
[5] J. I. Cunneen, *J. Chem. Soc.* **1947**, 134–141.
[6] M. Preisenberger, A. Schier, H. Schmidbaur, *J. Chem. Soc. Dalton Trans.* **1999**, 1645–1650.
[7] M. D. Nyman, M. J. Hampden-Smith, E. N. Duesler, *Inorg. Chem.* **1997**, *36*, 2218–2224.
[8] W. A. Sheppard, E. L. Muetterties, *J. Org. Chem.* **1960**, *25*, 180–182.
[9] W. V. Rochat, G. L. Gard, *J. Org. Chem.* **1969**, *34*, 4173–4176.
[10] W. Gordy, *J. Chem. Phys.* **1946**, *14*, 560–562.
[11] H. S. Randhawa, C. N. R. Rao, *J. Mol. Struct.* **1974**, *21*, 123–134.
[12] H. S. Randhawa, W. Walter, C. O. Meese, *J. Mol. Struct.* **1977**, *37*, 187–192.
[13] E. A. Noe, *J. Am. Chem. Soc.* **1977**, *99*, 2803–2805.
[14] R. M. Romano, C. O. Della Védova, A. J. Downs, *J. Phys. Chem. A* **2002**, *106*, 7235–7244.
[15] S. Nagata, T. Yamabe, K. Fukui, *J. Phys. Chem.* **1975**, *79*, 2335–2340.
[16] M. F. Erben, M. Geronés, R. M. Romano, C. O. Della Védova, *J. Phys. Chem. A* **2006**, *110*, 875–883.
[17] K. I. Gobbato, C. O. Della Védova, H. G. Mack, H. Oberhammer, *Inorg. Chem.* **1996**, *35*, 6152–6157.
[18] G. A. Crowder, *Appl. Spectrosc.* **1973**, *27*, 440–443.
[19] H. Møllendal, *J. Phys. Chem. A* **2007**, *111*, 1891–1898.
[20] M. F. Erben, C. O. Della Védova, H. Willner, R. Boese, unpublished results.
[21] M. F. Erben, C. O. Della Védova, H. Willner, R. Boese, *Eur. J. Inorg. Chem.* **2006**, *21*, 4418–4425.
[22] M. F. Erben, C. O. Della Védova, H. Willner, F. Trautner, H. Oberhammer, R. Boese, *Inorg. Chem.* **2005**, *44*, 7070–7077.
[23] J. W. Martin, J. Franklin, M. L. Hanson, K. R. Solomon, S. A. Mabury, D. A. Ellis, B. F. Scott, D. C. G. Muir, *Environ. Sci. Technol.* **2000**, *34*, 274–281.
[24] J. R. Durig, J. F. Davis, G. A. Guirgis, *J. Mol. Struct.* **1994**, *328*, 19–35.
[25] K. I. Gobbato, C. Leibold, S. Centeno, C. O. Della Védova, H.-G. Mack, H. Oberhammer, *J. Mol. Struct.* **1996**, *380*, 55–61.
[26] D. W. Deerfield II, L. G. Pedersen, *J. Mol. Struct. (THEOCHEM)* **1995**, *358*, 99–106.
[27] H. M. Badawi, *Spectrochim. Acta, Part A* **2004**, *60*, 2573–2580.
[28] S. E. Ulic, K. I. Gobbato, C. O. Della Védova, *J. Mol. Struct.* **1997**, *407*, 171–175.
[29] G. A. Crowder, E. Robertson, K. Potter, *Can. J. Spectrosc.* **1975**, *20*, 49–51.
[30] D. W. Scott, M. Z. El-Sabban, *J. Mol. Spectrosc.* **1969**, *30*, 317–337.
[31] A. B. Dempster, G. Zerbi, *J. Mol. Spectrosc.* **1971**, *39*, 1–7.
[32] G. C. Cole, H. Møllendal, J.-C. Guillemin, *J. Phys. Chem. A* **2006**, *110*, 9370–9376.
[33] A. C. Fantoni, W. Caminati, *J. Mol. Spectrosc.* **1990**, *143*, 389–391.
[34] G. C. Cole, H. Møllendal, B. Khater, J.-C. Guillemin, *J. Phys. Chem. A* **2007**, *111*, 1259–1264.
[35] A. Bondi, *J. Phys. Chem.* **1964**, *68*, 441–451.
[36] W. Mikenda, E. Steinwender, K. Mereiter, *Monatsh. Chem.* **1995**, *126*, 495–504.
[37] O. Niyomura, S. Kato, *Top. Curr. Chem.* **2005**, *251*, 1–12.
[38] M. Schilling, D. Mootz, *J. Fluorine Chem.* **1995**, *74*, 255–258.
[39] J. R. Durig, H. V. Phan, J. A. Hardin, T. S. Little, *J. Chem. Phys.* **1989**, *90*, 6840–6851.
[40] J. R. Durig, W. Zhao, D. Lewis, T. S. Little, *J. Chem. Phys.* **1988**, *89*, 1285–1296.
[41] G. A. Guirgis, H. Phan, J. F. Davis, J. R. Durig, *J. Mol. Struct.* **1993**, *293*, 11–14.
[42] J. R. Durig, M. Mamula Bergana, H. V. Phan, *J. Mol. Struct.* **1991**, *242*, 179–205.
[43] P. T. Brain, D. W. H. Rankin, H. E. Robertson, M. Buhl, *J. Mol. Struct.* **1996**, *376*, 123–132.
[44] M. F. Erben, C. O. Della Védova, R. Boese, H. Willner, H. Oberhammer, *J. Phys. Chem. A* **2004**, *108*, 699–706.
[45] J. H. M. ter Brake, R. A. J. Driessen, F. C. Mijlhoff, G. H. Renes, A. H. Lowrey, *J. Mol. Struct.* **1982**, *81*, 277–282.

[46] Q. Shen, R. Krisak, K. Hagen, *J. Mol. Struct.* **1995**, *346*, 13–19.
[47] M. F. Erben, C. O. Della Védova, R. M. Romano, R. Boese, H. Oberhammer, H. Willner, O. Sala, *Inorg. Chem.* **2002**, *41*, 1064–1071.
[48] C. O. Della Védova, R. M. Romano, H. Oberhammer, *J. Org. Chem.* **2004**, *69*, 5395–5398.
[49] A. Hermann, S. E. Ulic, C. O. Della Védova, M. Lieb, H.-G. Mack, H. Oberhammer, *J. Mol. Struct.* **2000**, *556*, 217–224.
[50] M. F. Erben, R. Boese, C. O. Della Védova, H. Oberhammer, H. Willner, *J. Org. Chem.* **2006**, *71*, 616–622.
[51] L. Leiserowitz, *Acta Crystallogr., Sect. B* **1976**, *32*, 775–802.
[52] P.-G. Jönsson, *Acta Crystallogr., Sect. B* **1971**, *27*, 893–898.
[53] F. H. Allen, W. D. S. Motherwell, P. R. Raithby, G. P. Shields, R. Taylor, *New J. Chem.* **1999**, *23*, 25–34.
[54] W. Gombler, H. Willner, *J. Phys. E* **1987**, *20*, 1286–1288.
[55] D. Brodalla, D. Mootz, R. Boese, W. Oßwald, *J. Appl. Crystallogr.* **1985**, *18*, 316–319.
[56] R. Boese, M. Nussbaumer, *In Situ Crystallisation Techniques* in *Organic Crystal Chem.*, vol. 7 (Ed.: D. W. Jones), Oxford University Press, Oxford, **1994**, p. 20.
[57] *SHELTX-Plus*, version SGI IRIS Indigo, a Complex Software Package for Solving, Refining and Displaying Crystal Structures, Siemens, Germany, **1991**.
[58] M. J. Frisch, G. W. Trucks, H. B. Schlegel, G. E. Scuseria, M. A. Robb, J. R. Cheeseman, J. A. Montgomery Jr, T. Vreven, K. N. Kudin, J. C. Burant, J. M. Millam, S. S. Iyengar, J. Tomasi, V. Barone, B. Mennucci, M. Cossi, G. Scalmani, N. Rega, G. A. Petersson, H. Nakatsuji, M. Hada, M. Ehara, K. Toyota, R. Fukuda, J. Hasegawa, M. Ishida, T. Nakajima, Y. Honda, O. Kitao, H. Nakai, M. Klene, X. Li, J. E. Knox, H. P. Hratchian, J. B. Cross, C. Adamo, J. Jaramillo, R. Gomperts, R. E. Stratmann, O. Yazyev, A. J. Austin, R. Cammi, C. Pomelli, J. W. Ochterski, P. Y. Ayala, K. Morokuma, G. A. Voth, P. Salvador, J. J. Dannenberg, V. G. Zakrzewski, S. Dapprich, A. D. Daniels, M. C. Strain, O. Farkas, D. K. Malick, A. D. Rabuck, K. Raghavachari, J. B. Foresman, J. V. Ortiz, Q. Cui, A. G. Baboul, S. Clifford, J. Cioslowski, B. B. Stefanov, G. Liu, A. Liashenko, P. Piskorz, I. Komaromi, R. L. Martin, D. J. Fox, T. Keith, M. A. Al-Laham, C. Y. Peng, A. Nanayakkara, M. Challacombe, P. M. W. Gill, B. Johnson, W. Chen, M. W. Wong, C. Gonzalez, J. A. Pople, *Gaussian 03*, *Revision B.04*, Gaussian, Inc., Pittsburgh, PA, **2003**.
[59] A. C. Scheiner, J. Baker, J. W. Andzelm, *J. Comput. Chem.* **1997**, *18*, 775–795.
[60] C. Peng, P. Y. Ayala, H. B. Schlegel, M. J. Frisch, *J. Comput. Chem.* **1996**, *17*, 49–56.
[61] L. Hedberg, I. M. Mills, *J. Mol. Spectrosc.* **2000**, *203*, 82–95.
[62] R. S. Corley, S. G. Cohen, M. S. Simon, H. T. Wolosinski, *J. Am. Chem. Soc.* **1956**, *78*, 2608–2610.

Received: April 19, 2007
Published Online: July 30, 2007

